The Journal of Experimental Biology 207, 3483-3494
Published by The Company of Biologists 2004
doi:10.1242/jeb.01170

The buccal buckle: the functional morphology of venom spitting in cobras

Bruce A. Young*, Karen Dunlap, Kristen Koenig and Meredith Singer

Department of Biology, Lafayette College, Easton, PA 18042, USA

*Author for correspondence at present address: School of Biological Sciences, PO Box 664236, Washington State University, Pullman, WA 99164-4236, USA (e-mail: youngb@wsu.edu)

Accepted 5 July 2004

Summary

Multiple radiations of Asiatic and African cobras have independently evolved the ability to expel their venom as a pressurized horizontal stream, a behavior commonly referred to as spitting. Though the unique fang morphology of spitting cobras is well known, the functional bases of venom spitting have received little attention. The combined results of gross and microscopic morphology, high-speed digital videography, experimental manipulations of anesthetized cobras and electromyography reveal a two-part mechanism for spitting venom. Contraction of the M. protractor pterygoideus (PP) causes displacement and deformation of the palato-maxillary arch and fang sheath; ultimately this displacement removes soft tissue barriers to venom flow that are normally present within the fang sheath. The M. adductor mandibulae externus superficialis (AMES) is activated simultaneously with the PP; the AMES increases venom pressure within the venom gland, propelling a stream of venom through the venom duct and out the fang. The displacements of the palato-maxillary arch, which form the first part of the spitting mechanism, are very similar to the motions of these bones during prey ingestion (the pterygoid walk), suggesting that venom spitting may have evolved from a specialization of prey ingestion, rather than prey capture.

Key words: snake, reptile, fluid pressure, dentition, defensive behavior, venom.

Introduction

Snakes exhibit a wide range of passive and active defensive behaviors (for reviews, see Carpenter and Ferguson, 1977; Greene, 1988). A specialized active defensive behavior, the ability to spit venom at a harasser or potential predator, is found in several species of African and Asiatic cobras. Though the phylogenetics of spitting and non-spitting cobras are not fully resolved, current evidence suggests that the ability to spit venom has evolved multiple times (e.g. Wüster, 1996; Slowinski et al., 1997; Keogh, 1998). Among spitting cobras there is considerable variation in the distance covered by the spat venom and the prevalence of associated defensive behaviors such as lunging (Rasmussen et al., 1995). Though experimental evidence is currently lacking, the spit is generally described as being aimed at the eyes of the harasser or predator; if even a small quantity of venom contacts the eye it produces intense pain and disruption of the cornea (Warrell and Ormerod, 1976; Ismail et al., 1993).

Some cobras can spit their venom as far as 3 m; the fluid pressures required to propel venom that far were explored by Freyvogel and Honegger (1965). Rosenberg (1967) described how venom pressure could be generated by the contraction of the skeletal muscles that contact the venom gland. This aspect of venom expulsion mechanics has been supported by experimental studies of rattlesnakes (Young et al., 2000). Through direct measurement of venom flow coupled with high-speed digital videography, a new model for the mechanics of venom expulsion has been developed (Young et al., 2002). This new model, termed the pressure-balance model, emphasizes the functional significance of the soft-tissue structures in the distal portion of the venom delivery system near the fang sheath.

Recent experimental work has demonstrated that displacement of the fang sheath towards the base of the fang, as well as pressure changes in the venom delivery system, can significantly influence venom flow (Young et al., 2001a, 2003). In most venomous snakes physical displacement of the fang sheath, either by a container during milking or by the target surface during fang penetration, is a prerequisite for venom release. Spitting cobras appear to be unique among venomous snakes in their ability to expel their venom without making direct physical contact with another object or organism. The classic description of the mechanics of venom spitting in cobras (Bogert, 1943) emphasized the specialized exit orifice of the fang of spitting cobras. The exit orifice (Fig. 1) of spitting cobras is directed more craniad and has a more circular aperture than the exit orifice of non-spitting cobras. These dentitional specializations explain how the venom stream expelled by spitting cobras travels forward,

rather than downward, but do not explain how the venom is expulsed without physical contact. The goal of this study was to test the hypothesis that venom spitting in cobras is dependent on deformation of the fang sheath and thus is functionally convergent with the venom delivery mechanics of crotalids.

Materials and methods

Live animals

This study was based on observations and experimentation involving five Black-necked spitting cobras *Naja nigricollis* Reinhardt (snout–vent length, *SVL*=45–130 cm); one Red spitting cobra *Naja pallida* Boulenger (*SVL*=89 cm); one Indochinese spitting cobra *Naja siamensis* Laurenti (*SVL*=122 cm); four Egyptian cobras *Naja haje* L. (*SVL*=145–173), and three Forest cobras *Naja melanoleuca* Hallowell (*SVL*=35–50 cm). All specimens were obtained commercially and maintained at Lafayette College in a special venomous snake room at 27–31°C, with a 12 h:12 h light cycle, water *ad libitum*, and a diet of pre-killed rodents. The snakes were not fed within 1 week of any surgical procedure, and care was taken to minimize the amount of venom spat during routine handling. Maintenance and use of these animals followed guidelines for reptiles and particularly venomous snakes, and all experimental protocols were approved by the Institutional Animal Care and Use Committee of Lafayette College.

Fig. 1. Scanning electron micrographs of the exit orifice of a non-spitting cobra *Naja kaouthia* (left) and a spitting cobra *Naja pallida* (right). Note the differences in the shape of the exit orifice.

High-speed videography and photography

Multiple spitting episodes (at least five episodes each for two *N. nigricollis*, and one each of *N. pallida* and *N. siamensis*) were recorded using a MotionScope 1000S (Redlake Instruments) at 500 frames s^{-1} with a 1/2000 s shutter speed. The digital record was then streamed to a G4 computer (Apple) and saved using Premiere 6.5 (Adobe). Subsequent quantification of the temporal pattern of the spit and jaw angles were performed using N.I.H. Image 1.6.3. Every spitting and non-spitting cobra was photographed during different forms of venom expulsion (milking, striking and spitting).

Observations

Our analyses of live specimens were augmented by standard video recordings of over 700 spitting episodes (detailed in Rasmussen et al., 1995), which include footage of *N. nigricollis*, *N. mossambica*, *N. pallida*, *N. siamensis* and *Hemachatus haemachatus* Lacepede. As part of an earlier study of spitting cobra venom (Cascardi et al., 1999), B.A.Y. maintained seven adult *Naja pallida*, which were regularly induced to spit. The prey ingestion and transport sequence of these snakes was videotaped by Alexandra Deufel (Deufel and Cundall, 2004) who was kind enough to provide us with a copy of the video footage.

Anatomy

To understand the anatomical basis of spitting in cobras, we examined the gross and microscopic morphology of the venom apparatus of a number of species. We examined prepared skulls of *N. naja* (Museum of Comparative Zoology, MCZ 4038); *N. nigricollis* (MCZ 53505, 53740; Field Museum of Natural History, FMNH 98910, and United States National Museum, USNM 320722); *N. melanoleuca* (FMNH 31364, USNM 320711), as well as one skull of *N. pallida* from the private collection of B.A.Y. Gross dissection was performed on the venom delivery systems of preserved adult specimens of *N. nigricollis* (MCZ 18477, USNM 40991), *N. melanoleuca* (FMNH 191427, MCZ 49688, USNM 49013), as well as the following species from the private collection of B.A.Y. (*Naja kaouthia*, *N. naja*, *N. nigricollis*, *N. nivea*, *N. pallida* and *H. haemachatus*).

As part of an earlier study (Young et al., 2001b) of the comparative microscopic anatomy of the distal venom delivery system in snakes, the head and several anterior vertebrae were removed from previously preserved elapid specimens (*Boulengerina annulata*, *Hemachatus haemachatus*, *Naja nigricollis* and *N. sputatrix*) and placed in decalcifying solution (Cal-Ex, Fisher, Pittsburgh, USA) for 72–168 h. Following decalcification, each head was bisected sagitally and tissues caudal to the midpoint of the venom gland were discarded. Each sample was dehydrated and cleared through a progressive ethanol series and Hemo-De (Fisher) prior to embedding in Paraplast (Fisher). Serial sections were cut at 10 μm, with one side of the head being sectioned parasagitally and the other sectioned frontally. Sections were stained using either Van Gieson's stain or Masson's Trichrome stain (following Luna,

1968; Presnell and Schreibman, 1997), which provide clear distinction between connective tissue, muscle and epithelium, and then were examined and photographed using an E800M compound microscope (Nikon, Melville, USA). Additional observations were made on serial sections through the head of *Walterinnesia aegyptia* kindly provided by Elazar Kochva.

Fully ankylosed, functional fangs were removed from preserved adult specimens of *N. kaouthia* and *N. pallida* from the private collection of B.A.Y. The fangs were air-dried prior to being critical-point-dried (Polaron, Watford, UK), and coated with 300 Å of gold (PS-2, International Scientific Instruments, Prahan, Australia). The fangs were examined and photographed at 15 kV using a Super-3A scanning electron microscope (International Scientific Instruments).

Stimulation and strain gauges

To explore the mechanical role of the M. protractor pterygoideus in spitting, we anesthetized (*via* exposure to isoflurane and an intramuscular injection of 65 mg kg^{-1} ketamine hydrochloride:acepromazine in a 9:1 ratio) an adult specimen of *N. siamensis* and surgically exposed this muscle unilaterally. A bipolar stimulating probe was applied to the surface of the muscle and a range of electrical stimulations were presented using an S88 Stimulator (GRASS, West Warwick, USA). To better document the resultant changes, these stimulations were repeated following the attachment (*via* Vetbond; Sarasota, USA) of a uniaxial strain gauge (EA-13-062AK-120, Measurements Group, Raleigh, USA) on the oral mucosa of the roof of the mouth immediately below, and parallel to the long axes of, the maxilloectopterygoid and palatopterygoid joints. The strain gauge was coupled to a P122 amplifier (GRASS) and the signal from the amplifier, along with a synch pulse from the stimulator, was transferred to a G4 computer (Apple) at 20 kHz sampling rate using the Instrunet data acquisition system (G.W. Instruments, Somerville, USA) and quantified using SuperScope (G.W. Instruments).

A second uniaxial strain gauge was attached (with Vetbond) to the dorsal scales over, and parallel to the long axis of, the nasofrontal joint of an adult *N. nigricollis* that had been lightly anesthetized through inhalatory exposure of isoflurane. When the snake was fully recovered from the anesthesia it was placed unrestrained in an open container 75 cm×75 cm×50 cm tall. The strain gauge signal was amplified and recorded as above; one of the experimenters induced the cobra to spit and depressed a remote switch to generate a marker voltage, which was recorded by the computer simultaneously with the strain gauge output.

Venom pressure

Venom pressure was measured at two sites on two adult specimens of *N. nigricollis*. Each snake was anesthetized as described above, then placed on a heated surgical table (VSSI) and maintained on isoflurane using a low-flow ventilator (Anesco, Waukesha, USA). A small rotary tool was used to remove the end of the fang proximal to the exit orifice, then a 60 cm length of polyethylene (PE) tubing was placed over the fang. The inner diameter of the PE tubing was such that a tight fit was achieved with the outer surface of the fang. The free end of the PE tubing was attached to a PT300 pressure transducer (GRASS), and both were filled with Ringer's solution. The M. protractor pterygoideus and M. adductor mandibulae externus superficialis were then surgically exposed. Using a dual bipolar probe and the S88 Stimulator (GRASS), each muscle was stimulated individually, then the two muscles were stimulated simultaneously. During the stimulations the exit port of the pressure transducer was sealed so that the transducer formed a closed system that would not dissipate venom when pressurized. The pressure transducer was coupled to a P122 amplifier (GRASS), and the final signal, along with a synchronized pulse from the stimulator, was captured by the data acquisition system as described above.

In an effort to determine the influence of the soft tissues of the distal end of the venom delivery system, venom pressures were also recorded from the proximal portion of the venom duct. For this preparation, a portion of the venom duct was surgically isolated from the surrounding connective tissue, vasculature and supralabial gland. A small incision was made on the lateral surface of the venom duct and a PE tubing catheter was inserted into the lumen of the duct. Silk suture was used to anchor the catheter in place and to prevent venom leakage around the catheter. In both preparations the muscles received at least 5 twitch stimuli (1 stimulus every 2 s, 15 ms duration, 8 V) as well as one or two train stimuli (35 p.p.s., 27 ms duration, 8 V).

Electromyography

Two adult specimens of *N. nigricollis* were used for the EMG experiments. The animals were anesthetized with isoflurane and two small incisions made in the dorsal scales of the head. Bipolar EMG electrodes 1 m in length were fashioned from 0.05 mm diameter stainless steel wire with nylon insulation (California Fine Wire, Grover Beach, USA), and inserted into either the M. protractor pterygoideus or M. adductor mandibulae externus superficialis using hypodermic needles. The incisions were closed with silk suture and Vetbond, and the EMG leads were glued to one another and to a tether of suture anchored to the dorsal midline of the snake's neck.

With the leads in place, and the cobra recovering from anesthesia, the snake was placed in a clear acrylic tube 50 cm long such that the anterior and posterior ends of the snake projected beyond the tube. This tube allowed us to safely restrain the snake (by holding the posterior body); though the snake had full movement of its head and neck, it had reduced opportunities to damage the EMG leads. With the snake restrained in this fashion, the EMG leads were coupled to two P511 amplifiers (GRASS), which were coupled to the data acquisition system as described above and sampled at 33 kHz. We built a spit detector to generate a marker on our computer records. This detector was constructed from a 15 cm^2 plate of Plexiglas onto which we laid intermeshed strips of copper tape with only 1 mm gap between them. Alternate strips were wired

to either the anode or cathode of a 6 V battery, with the termini connected to the data acquisition system. The cobra was induced to spit by one of the experimenters; if the spit detector was held in front of the experimenter's face (which the cobra targets) the venom striking the detector would form a complete circuit, sending a pulse to the data acquisition system.

Results

High-speed videography and photography

High-speed digital videography revealed that the spitting behavior had consistent patterns of kinematics, both in the spat fluid and the cobra's head. The spat venom stream exhibited an initial pressurization phase, during which the stream started out almost ventrad, then rapidly (<10 ms) arced up to the typical trajectory, which was slightly inclined above the horizontal. The termination of the spit showed a corresponding decrease in venom pressure as the spit stream arced ventrad.

The spit was always released with the mouth slightly open, typically around 25° (mean ± S.E.M. = 22.6±2.5°, *N*=16); as the venom was released the gape would decrease slightly then increase again. Immediately prior to the onset of venom expulsion, four concurrent displacements were observed in the skull. First, the snout complex rotated in the sagittal plane such that the tip of the snout was elevated relative to the resting position. Second, the caudal end of the maxilla was displaced laterally causing a bulge or deformation of the overlying supralabial scales (Fig. 2A). Third, the fang sheath, the drape of connective tissue and epithelium surrounding the fang, elevated to expose the fang tip. Lastly, two ventrally directed projections appeared in the oral mucosa of the roof of the mouth. These projections occurred side by side, with a slight gap between them, at a level slightly caudal to the scale bulge associated with the maxilla. The palatal bulges were particularly evident if the cobra was filmed from a slightly ventral perspective (Fig. 2B).

With the cobras anesthetized prior to the surgical procedures, force was applied manually to the quadratopterygoid articulation in an attempt to protract the palato-maxillary arch. This manipulation produced the same suite of displacements observed within the skull during spitting, though the projections of the palatal mucosa were not as pronounced.

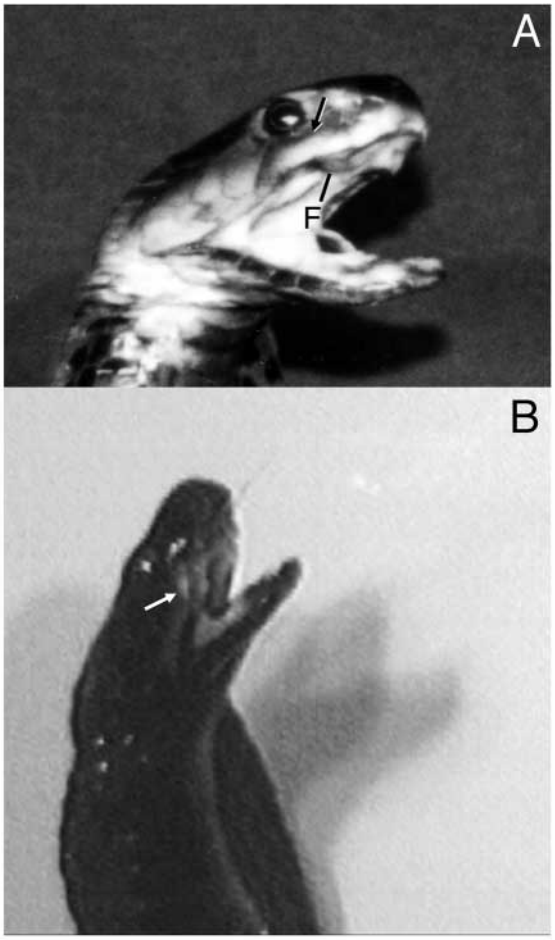

Fig. 2. Deformations of the palato-maxillary arch during spitting. (A) *Naja nigricollis* immediately prior to spitting; note the deformation of the supralabial scales (arrow) caused by the frontal rotation of the maxilla; (B) a high-speed digital videograph recording of *N. nigricollis* spitting; note the ventral projections on the roof of the mouth (arrow). F, fang.

Observations

The slower frame rate of the standard video recordings of spitting made it more difficult to discern all of the kinematic features. Nevertheless, the displacements described above appeared to be a consistent feature of the spitting behavior of every species. These same displacements were absent from the video recordings of other venom expulsion events (such as milking or prey capture) involving both spitting and non-spitting cobras. The palato-maxillary displacement associated with prey ingestion, the well-known 'pterygoid walk' of snakes (see Boltt and Ewer, 1964; Deufel and Cundall, 2004), was evident in video sequences of *N. pallida*; however, these displacements were distinct from those observed during spitting. The suite of displacements that was consistently observed during spitting was never observed in non-spitting cobras, nor was it recorded from spitting cobras engaged in any other behavior, including other forms of venom expulsion.

Anatomy

A detailed description of the cephalic morphology of *Naja* is beyond the scope of this contribution (see Radovanovic, 1928; Haas, 1930, 1973; Deufel and Cundall, 2004), the following is intended only as a general orientation. The upper jaw, or palato-maxillary arch, of cobras consists of four bones, the pterygoid, ectopterygoid, palatine and maxilla. The dentiferous pterygoid, the caudal element in the series, is a horizontal bar of bone, the caudal end of which deflects laterad and becomes more spatulate (Fig. 3). The proximal end of the non-dentiferous ectopterygoid has an elongate but poorly defined articulation on the dorsal surface of the pterygoid. The

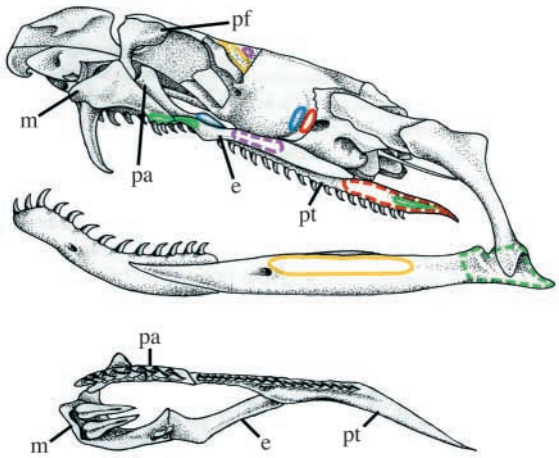

Fig. 3. Illustration of the lateral view of the skull, and ventral view of the palato-maxillary arch, of *Naja nigricollis*. Muscle attachment sites are shown as solid colors (lateral surface) or broken colors (medial surface) for the following muscles: M. adductor mandibular externus superficialis (yellow); M. levator pterygoideus (purple); M. protractor pterygoideus (red); M. retractor pterygoideus (blue); M. pterygoideus (green). e, ectopterygoid; m, maxilla; pa, palatine; pf, prefrontal; pt, pterygoid.

ectopterygoid extends craniolaterally with a slight dorsal deflection; the distal end of the ectopterygoid is a broad, horizontal plate of bone (Fig. 3). The caudal end of the dentiferous palatine abuts the cranial tip of the pterygoid; from here the palatine extends craniolaterally to approach the cranial tip of the maxilla (Fig. 3). The cranial end of the palatine supports a large medial process that has a connective tissue link to the frontals, and a lateral process that is bound (*via* connective tissue) to the maxilla and prefrontal; the cranial tip of the palatine has a connective tissue attachment to the overlying ventral portions of the snout complex (vomer, septomaxilla and nasal). The caudal end of the maxilla rests under the distal end of the ectopterygoid (Fig. 3); the medial portion of this contact is heavily imbued with dense connective tissue while the lateral portion has a more complex articulation and less connective tissue. Distally the maxilla supports a medial process that contacts the palatine, and the dorsal surface of the maxilla has an extensive articulation with the distal end of the prefrontal (Fig. 3).

Four skeletal muscles contact the palato-maxillary arch. The M. protractor pterygoideus originates from the caudolateral

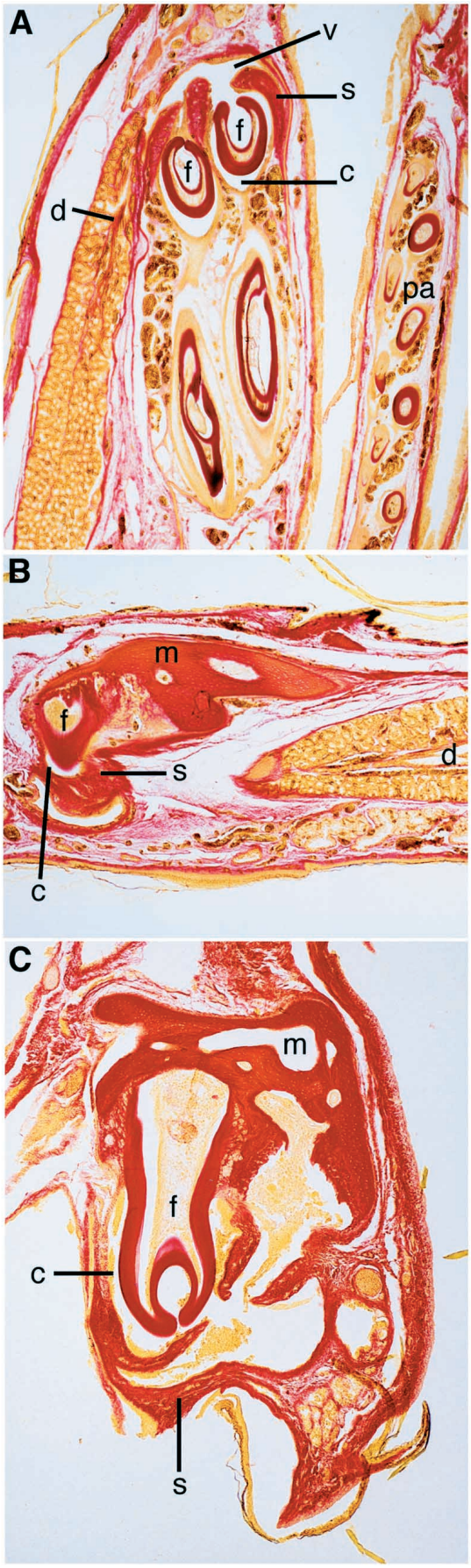

Fig. 4. Histology of the distal venom delivery system. (A) Frontal section of a spitting cobra *Naja sputatrix* showing the soft tissue chambers within the fang sheath. (B) Parasagittal section through *N. sputatrix* showing the venom duct approaching the lateral margin of the fang sheath. (C) Transverse section through the fang sheath of a non-spitting cobra *N. melanoleuca* illustrating the links between the fang sheath and the maxilla and the internal partitions of the fang sheath. c, venom chamber; d, venom duct; f, fang; m, maxilla; pa, palatine; s, fang sheath; v, venom vestibule.

surface of a prominent ridge, which forms the caudolateral portion of the suture between the parietal and basisphenoid bones, and inserts on the caudal two-thirds of the pterygoid (Fig. 3). The M. levator pterygoideus originates from the lateral surface of the skull and the postorbital fossa (at a point cranial and dorsal to that of the protractor) and inserts on the pterygoid near the pterygoidoectopterygoid joint (Fig. 3). The M. retractor pterygoideus originates immediately cranial to the protractor, from the craniolateral surface of the parietobasisphenoid ridge, and inserts on the cranial tip of the pterygoid and the caudal palatine (Fig. 3). The largest of these four muscles, the M. pterygoideus, originates from the caudal end of the compound bone of the lower jaw and the adjacent caudolateral surface of the pterygoid, and inserts onto the distal end of the ectopterygoid and the connective tissue surrounding the maxilloectopterygoid joint (Fig. 3).

The fang and replacement fang are surrounded by a drape of connective tissue and epithelium termed the fang sheath (Fig. 4). The fang sheath is devoid of smooth and skeletal muscle tissue. The dorsal margin of the fang sheath is attached to the lateral and cranial surfaces of the maxilla (Fig. 4) as well as the adjacent oral mucosa. The venom duct is closely attached to the lateral surface of the maxilla. The caudolateral surface of the fang sheath is penetrated by the venom duct, which continues to course craniad within the fang sheath. At the cranial surface of the maxilla the venom duct expands in width and arches medially to form the venom vestibule (Fig. 4). The caudal margin of the venom vestibule supports two distinct foramina. These foramina extend caudally to a venom chamber, which surrounds each fang (Fig. 4). The epithelial linings of the venom chambers, the foramina and the venom vestibule are continuous with that of the venom duct (Fig. 4). This distal portion of the venom delivery system is devoid of skeletal muscle; these soft tissue chambers are contained entirely within the fang sheath.

A comparison of the gross and histologic morphology of the palato-maxillary arch among spitting (mainly *H. haemachatus*, *N. nigricollis* and *N. pallida*) and non-spitting (mainly *N. melanoleuca*, *N. naja* and *Walterinessia aegyptia*) cobras revealed only minor differences beyond those at the fang's exit orifice (Fig. 1). The maxilla of non-spitting cobras was more horizontal at rest, the connective tissue asymmetry of the maxilloectopterygoid joint was more pronounced in spitting cobras, and the M. protractor pterygoideus appeared to be proportionately larger in spitting cobras (we lack the necessary series to quantify the latter observation). Neither these, nor the other subtle morphological differences we observed, appear to be a key morphological feature associated with the ability to spit venom.

Stimulation and strain gauges

In *N. siamensis* the contraction of the M. protractor pterygoideus, triggered by electric stimulation, produced displacements of the palato-maxillary arch that were clearly visible on the roof of the mouth (Fig. 5). The maxilla was protracted and rotated in the frontal plane such that the caudal end of the maxilla moved laterally. The palatine is protracted, though seemingly not as much as the maxilla, and appears to rotate in the frontal and sagittal plane (the caudal palatine teeth become exposed while the anteriormost are not). There is a ventral buckling of the palato-maxillary arch in the region of the palatopterygoid joint and the maxilloectopterygoid joint. This buckling was manifest as two adjacent ventral protrusions from the palatal mucosa.

The displacement of the palatopterygoid and maxilloectopterygoid joints is evident in the signal obtained from the strain gauge attached to the oral mucosa under these joints (Fig. 6A). Twelve electrical stimulations of the M. protractor pterygoideus resulted in consistent voltage spikes from the strain gauge amplifier. The strain gauge attached to the dorsal scales over the nasofrontal joint of an unanesthetized *N. nigricollis* produced a clear pattern of deformation prior to each of 18 spits recorded (Fig. 6B). In this experiment the spit signal was triggered by the experimenter, and thus is delayed both by the time it takes the spit to reach the experimenter and the reaction time between spit contact and switch depression. Because no skeletal muscle contacts the snout complex of cobras, the only motive force for the rotary displacement of the snout is the palato-maxillary arch, and more specifically the palatine and maxilla.

Venom pressure

In *N. nigricollis*, when identical stimulation is applied to the same surface area of the M. protractor pterygoideus (PP) and the M. adductor mandibulae externus superficialis (AMES) individually or simultaneously, a clear pattern of changes in venom pressure is produced. Though the AMES is the only muscle directly contacting the venom gland, contractions of this muscle in isolation produce little venom pressure when

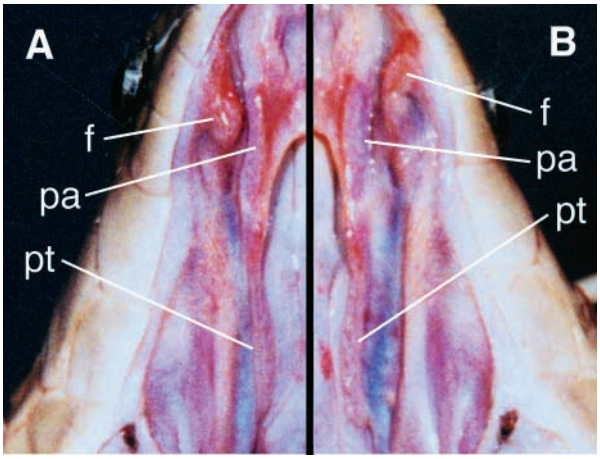

Fig. 5. Ventral view of the palate of an Indochinese spitting cobra *Naja siamensis* before (A) and after (B) stimulation of the M. protractor pterygoideus. Both A and B are photos of the same side of the same animal; B was transposed to enhance comparison. Note the protraction and rotations of the palato-maxillary arch. f, fang; pa, palatine; pt, pterygoid.

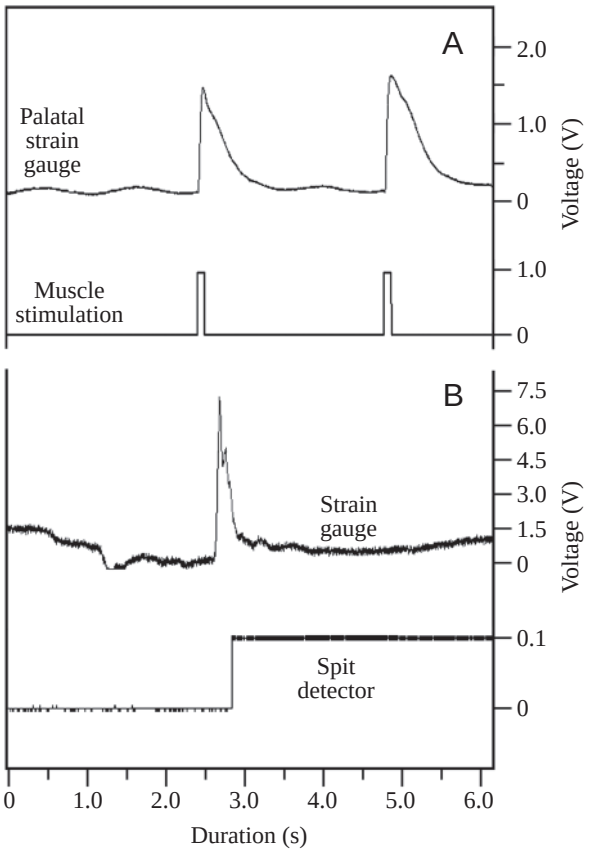

Fig. 6. Data tracings from two separate experiments in which strain gauges were placed on the palatal mucosa (A) or scales over the nasofrontal joint (B) of two separate spitting cobras *Naja nigricollis*. In both experiments contraction of the M. protractor pterygoideus, either artificially (A) or during spitting (B), resulted in deformations of the palato-maxillary arch evident in the strain gauge tracings.

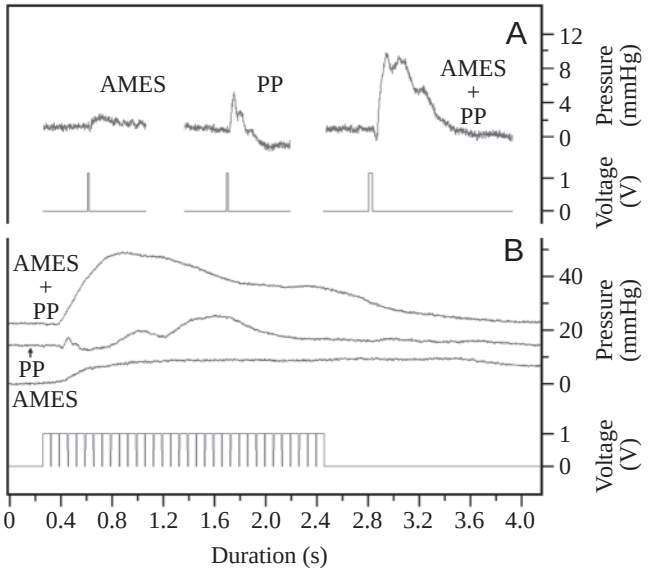

Fig. 7. Data tracings of venom pressure recorded from the fang tip of *Naja nigricollis*. Note that stimulation of the M. adductor mandibulae externus superficialis (AMES) simultaneously with the M. protractor pterygoideus (PP) produces greater venom pressure than when either is stimulated alone. This pattern holds whether the muscles are given twitch (A) or train (B) stimuli.

measured from the fang (Fig. 7A). The PP does not contact the venom gland or duct, but does produce displacement of the palato-maxillary arch and the soft tissues around the fang; stimulation of this muscle results in modest venom pressures at the fang tip, which are greater than those produced by the AMES (Fig. 7A). When the two muscles are stimulated together the resultant venom pressure at the fang tip is greater than the sum of the two individual stimulations, with combined venom pressures roughly double those produced by the PP alone (Fig. 7A). The 17 stimulation episodes produced the same pattern of relative contribution to venom pressure whether the muscle was exposed to a single twitch stimulus, or train stimuli (Fig. 7B).

When the pressure catheter is inserted into the proximal venom duct, thereby avoiding the soft tissue structures of the fang sheath, a markedly different pattern of venom pressures emerges. It is important to note that the twitch stimulations and the stimulated muscle areas used during the proximal pressure recordings were the same as those used for the distal recordings. Stimulation of the AMES produces a prominent spike of venom pressure (Fig. 8), which is roughly 200 times greater than that recorded from the fang tip. The high venom pressure produced by this stimulation, coupled with the closed recording system employed, resulted in long recovery times. Stimulation of the PP produced a pulse of venom pressure that was less than 10% that of the AMES and had a more rapid recovery time (Fig. 8). The venom pressure spike produced by stimulating the two muscles simultaneously was nearly identical to that produced by stimulating the AMES alone (Fig. 8). The additive effect that characterized the venom pressures recorded at the fang tip was not observed in the pressure tracings recorded more proximally.

Electromyography

Every spitting episode decreased the volume of venom in the venom gland, and thus could alter the forces acting on this system. To minimize this complication, we only recorded the first 15 spits produced by the cobras (some species can spit over 50 times; Rasmussen et al., 1995). The electrical activity of the muscles in *N. nigricollis* revealed a consistent pattern in every spit (Fig. 9). Nearly synchronous electrical activity was recorded from the M. protractor pterygoideus (PP) and the M. adductor mandibulae externus superficialis (AMES) immediately prior to the spit. The signals from the spit detector are delayed due, among other factors, to the time it takes the venom to travel from the fang to the spit detector. In one-third of the spits, a second low-level burst of activity was observed in the PP following the spit while the mouth was still open (Fig. 9), which we believe to be associated with a more subtle repositioning of the palato-maxillary arch following the spit.

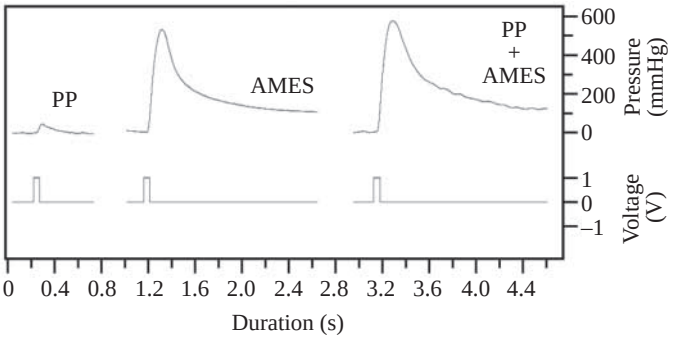

Fig. 8. Data tracings of venom pressure recorded from the venom duct of *Naja nigricollis*. Note that stimulation of the M. protractor pterygoideus (PP) had minimal influence on venom pressure, and there was no additive effect when stimulated simultaneously with the M. adductor mandibulae externus superficialis (AMES). Note the marked increase in venom pressures recorded at the venom duct compared to those recorded from the fang tip (Fig. 7).

The pattern of EMG activity during spitting was consistent in the two specimens of *N. nigricollis*. A series of spitting episodes from one of these specimens had been previously captured using high-speed videography. Quantitative analyses of these two data sets (using NIH Image for the video and SuperScope for the EMG signals) were performed to look for temporal patterns (Table 1). The quantitative features of the EMG signals presented in Table 1 are similar to those obtained from the second specimen of *N. nigricollis*; similarly, the spit durations presented below are similar to those observed in other specimens. Electrical activity in the PP precedes the activity in the AMES by 37 ms, and continues for 10 ms beyond the cessation of activity in the AMES (Table 1). The AMES, the compressor of the venom gland, is active for 96 ms during a spitting episode. Quantification of the high-speed digital records indicated a mean spit duration of 66 ms; this temporal measure of venom discharge includes the initial pressurization and terminal depressurization phases (Table 1). The onset of the palatal projections was clearly visible in 7 of the 12 spitting sequences captured from this specimen, and in these 7 sequences the palatal projections appeared 3 ms prior to the onset of spitting (Table 1).

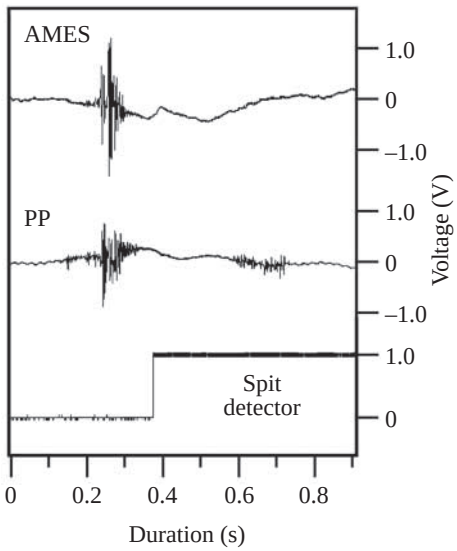

Fig. 9. Representative EMG tracing recorded when *Naja nigricollis* spat venom. Note the temporal congruence in the activity patterns of the M. adductor mandibulae externus superficialis (AMES) and the M. protractor pterygoideus (PP). Because the venom must travel from the fang to the detector, the signal from the spit detector is always delayed relative to the electrical activity within the muscles.

Table 1. *Quantitative aspects of the spitting behavior of* Naja nigricollis

	N	Mean	S.E.M.
Duration of spit	12	66	3.9
Duration of AMES activity	12	96	5.9
Duration of PP activity	12	143	8
Interval between PP and AMES onset	12	37	6.4
Interval between palatal displacement and venom expulsion	7	3	1

AMES, M. adductor mandibulae externus superficialis; PP, M. protractor pterygoideus.

Times are in ms.

Note that the quantitative features determined from electromyography and kinematics are from separate experiments on the same specimen.

Discussion

These analyses suggest that a two-component mechanism may form the functional basis of venom spitting in cobras. One component is displacement of the palato-maxillary arch; protraction coupled with some ventral flexion of the palatopterygoid and maxilloectopterygoid joints, and rotation of the maxilla in the frontal plane (Fig. 10). This displacement is produced by the actions of the M. protractor pterygoideus coupled with the arthrology of the maxilloprefrontal and maxilloectopterygoid joints. In terms of venom expulsion, the primary consequence of this palato-maxillary displacement is a dorsad translation and deformation of the fang sheath (Fig. 10). Ultimately this displacement of the fang sheath removes a physical barrier to venom expulsion. The second component of spitting is an increase in intraglandular pressure caused by contraction of the M. adductor mandibulae externus superficialis (Fig. 10). The increase in intraglandular pressure forces the venom from the venom gland through the venom duct, soft tissue chambers, and the venom fang. The elevated venom pressure propels the venom beyond the exit orifice of the fang as an airborne stream.

The results of our investigation support both components of this model for venom spitting. During the electromyography experiments, electrical activity was consistently recorded from the M. adductor mandibulae externus superficialis (AMES)

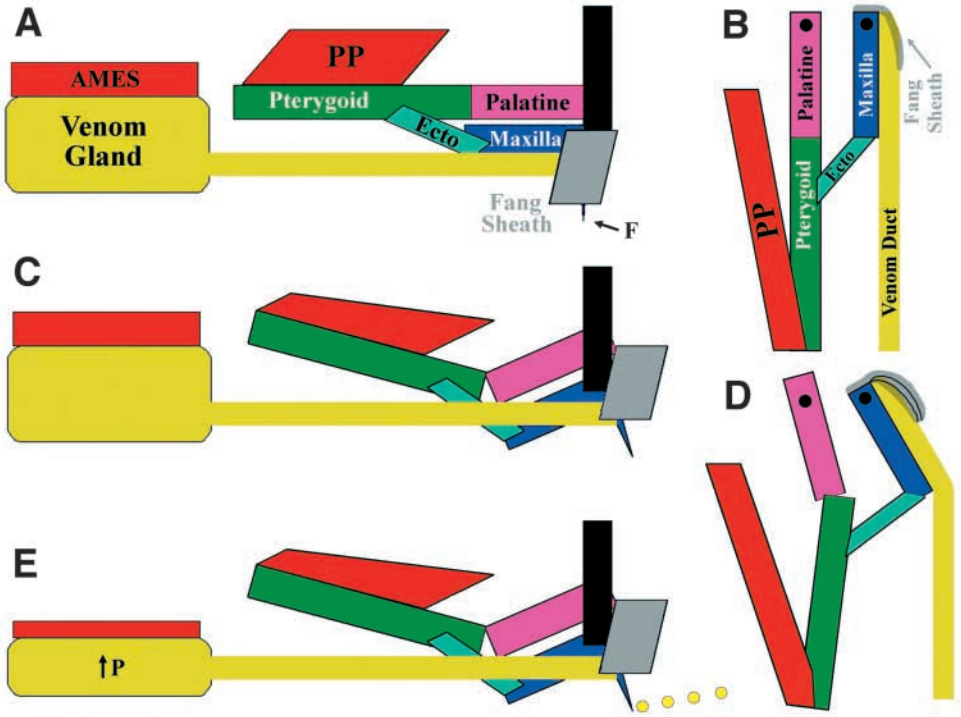

Fig. 10. Summary model for the mechanics of venom spitting. The palato-maxillary arch (comprising the pterygoid, palatine, ectopterygoid and maxilla) articulates with the skull at the prefrontal (black rectangle). Immediately adjacent to the palato-maxillary arch is the venom gland and duct; the fang sheath covers the anterior portion of the maxilla and venom duct. The system at rest is shown from a lateral (A) and dorsal (B) perspective. Upon contraction of the M. protractor pterygoideus (PP) the palato-maxillary arch is protracted, rotated in the sagittal plane (C), and rotated in the frontal plane (D). These rotations displace the fang sheath (D,E), removing barriers to venom flow such that when the M. adductor mandibulae externus superficialis (AMES) contracts, venom pressure can expel venom through the specialized exit orifice of the fang (E). P, pressure; F, fang.

immediately prior to the discharge of the spit (Fig. 9). Electrical stimulation of the AMES of anesthetized cobras produced an increase in venom pressure (Fig. 8). The other component of this model for spitting, the displacement of the palato-maxillary arch leading to a functional release of venom, was also supported by our experimental results. High-speed digital videography and photography of spitting cobras documented the displacement of the palato-maxillary arch immediately prior to the spit (Fig. 2). The displacement of the palato-maxillary arch was also evident in the results of the strain gauge experiments. The first experiment documented the direct displacement of the palatopterygoid and maxilloectopterygoid joints; the second experiment revealed the protraction and sagittal rotation of the palatine and maxilla by documenting the ensuing rotation of the snout complex (Fig. 6). The hypothesis that the M. protractor pterygoideus (PP) is responsible for the displacement of the palato-maxillary arch is supported by the findings that electrical stimulation of this muscle produce displacements similar to those observed during the venom spitting behaviors (Fig. 5), and that electromyographic signals were consistently recorded from this muscle immediately prior to the discharge of the venom stream (Fig. 9). One consequence of this palato-maxillary displacement was evident from the manipulation of anesthetized snakes, in which manual protraction of the palato-maxillary arch led to a dorsad translation of the fang sheath. The presence of a barrier to venom flow within the fang sheath is evident in the results of the pressure recordings. Venom pressures recorded distal to the venom barrier (at the fang tip) were approximately 1/200th of those recorded proximal to the venom barrier (from the venom duct) when the AMES was stimulated independently (Figs 7, 8). The PP, which produces deformation of the fang sheath, influences venom pressures recorded distal to the fang sheath (from the fang tip), but not those recorded proximal to the fang sheath. Other muscles in this region could also potentially influence venom expulsion; however, the spatial position, size and lever arms of the AMES and PP are such that they would have the greatest influence on venom flow.

This model for the functional basis of spitting does not directly speak to the relative timing of the two component parts. When sequential spits are considered (multiple spits are quite common in cobras; Rassmusen et al., 1995), three obvious temporal patterns are possible (Fig. 11). The M. adductor mandibulae externus superficialis (AMES) may have extended activity periods, thus keeping the venom gland pressurized, with periodic releases of venom associated with contraction of the M. protractor pterygroideus (PP). A second possible pattern is a close temporal coupling between the activity of the AMES and the PP, while the third involves asymmetrical activity of the PP extending beyond the termination of contraction of the AMES (Fig. 11). Cascardi et al. (1999) reported that *N. pallida* spat a rather consistent volume of venom in each spit, which is difficult to reconcile with protracted activity in the AMES. The high-speed videography of the venom stream revealed an initial pressurization phase, which also seems contrary to protracted contraction of the AMES. The results of the EMG experiments (Table 1) clearly support a close temporal coupling of the two muscles. The longer activation period of the PP presumably reflects the greater time and force needed to achieve displacement of the palato-maxillary complex, when compared

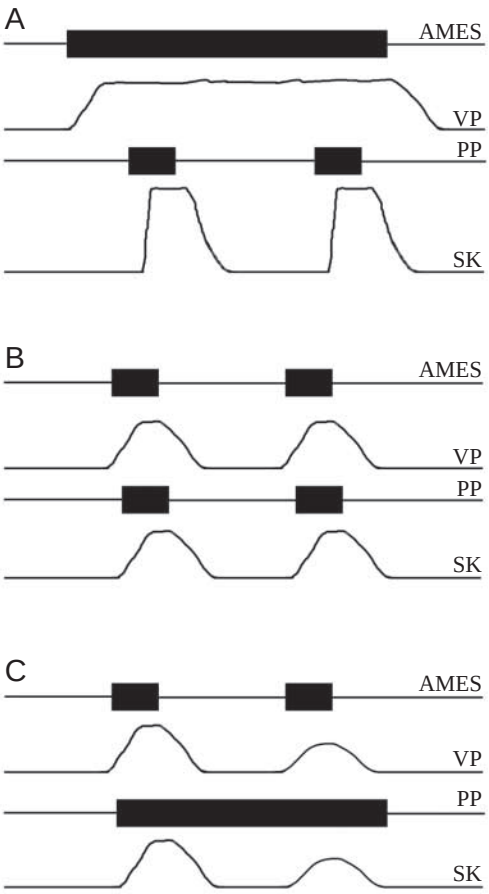

Fig. 11. Three hypotheses for the temporal pattern in the activation of the M. adductor mandibulae externus superficialis (AMES) and M. protractor pterygoideus (PP). (A) The AMES maintains a prolonged contraction resulting in sustained venom pressure (VP) within the venom gland; under this hypothesis the kinematics of the spit (SK) would be characterized by marked increases and decreases in venom flow. (B) Temporally congruent patterns in the AMES and PP, leading to congruent bell-shaped curves for venom pressure and spit kinematics. (C) Prolonged contraction of the PP with intermittent contract of the AMES, leading to variable patterns of venom pressure and spit kinematics.

to compression of the venom gland by the AMES. Though recorded separately, the temporal agreement between the duration of the spit and the duration of electrical activity in these muscles suggests a regular temporal coupling between these two muscles. In this view, multiple spits could be achieved in virtually any temporal pattern with dual activation of the muscles. Lastly, we saw no evidence of maintained displacement of the palato-maxillary arch in any of our cobras; prolonged displacement of the fang sheath, and the barriers to venom flow, would leave the cobra vulnerable to accidental discharge of venom during any movement of the lower jaw.

Rosenberg (1967) detailed the intra-glandular pressure model for venom injection in snakes, which described the functional relationship between contraction of the extrinsic venom gland musculature and venom expulsion. Key aspects of this model were supported by experimental studies of venom expulsion in *Crotalus* (Young et al., 2000), and by the results of the present study, where contraction of the extrinsic venom gland muscle (the AMES), either voluntarily by the cobra or through artificial stimulation, led to increases in venom pressure. Recently, Young et al. (2002) developed a refined and expanded model for venom expulsion, termed the pressure-balance model. This model emphasized the presence of passive barriers to venom flow, the morphology of the distal venom delivery system, and the role of the fang sheath in influencing venom flow. Simplistically, the pressure-balance model argues that venom pressure will build within the venom chambers of the fang sheath until physical displacement of the fang sheath, as during fang penetration, leads to venom flow through the fang (Young et al., 2002). A recent experiment has supported the pressure-balance model by showing that alterations of the peripheral resistance to venom flow have a significant impact on venom expulsion (Young et al., 2003). Spitting cobras were a natural test of the pressure-balance model in that, unlike apparently all other venomous snakes, they do not require direct physical contact with a target to release venom. The results of this study suggest that spitting cobras still utilize a pressure-balance system for venom expulsion; however, unlike all other venomous snakes where displacement of the fang sheath is passive, in spitting cobras the displacement is actively produced by the contraction of the M. protractor pterygoideus and the ensuing displacement of the palato-maxillary arch.

The results of the present study, when compared to earlier experimental analyses of the venom delivery mechanics in rattlesnakes, suggest that the venom delivery system of these two taxa (the Elapidae and Viperidae) have evolved independently and functionally converged. Nearly every aspect of the venom delivery system of elapids and viperids is morphologically distinct. The extrinsic venom gland musculature (see Haas, 1973; Jackson, 2003), venom gland and venom duct (see Gabe and Saint Girons, 1967; Kochva, 1978, 1987), maxilla and fangs (see Duvernoy, 1832; Knight and Mindell, 1994) and the venom chambers (Young et al., 2001b), all show marked morphological differences between elapids and viperids. Nevertheless, in both clades the extrinsic venom gland muscles function to raise intraglandular pressure, the venom chambers of the distal venom delivery system appear to pool venom and act as a barrier to venom flow, and displacement of the fang sheath appears to be a prerequisite to venom flow. Several scenarios (e.g. Savitzky, 1980; Kardong, 1982) have been proposed for the evolution of the venom delivery system in snakes; most commonly with a rear-fanged (opisthoglyphous) colubroid posited as the ancestral form of either viperids or elapids. Though the phylogeny of snakes remains uncertain, many recent morphological and/or molecular phylogenies have placed the viperids as basal within colubroid snakes (e.g. Pough et al., 1998). While the exact relationship of the different lineages within the colubroid snakes remains uncertain, there is general agreement that venom delivery systems evolved independently multiple times

within this radiation (see Jackson, 2003). The similarity between our findings and the earlier experimental study of the viperid *Crotalus* (principally Young et al., 2000, 2001a) suggests functional convergence between these two lineages.

The palato-maxillary arches of snakes exhibit varying kinematic patterns during prey capture and transport (Cundall and Greene, 2000). In viperids, protraction of the palato-maxillary arch produces rotation of the maxilla in both the sagittal and transverse planes, so that the width between the fangs is increased (Mitchell, 1861; Zamudio et al., 2000). Though more modest, the maxillae of some elapids have also been described as rotating in the transverse plane prior to envenomation (e.g. Fairley, 1929). The maxillary displacements we observed in *Naja* during spitting differ from previously described pre-envenomation motions in being composed of rotations in the frontal and sagittal planes, and in being most pronounced on the posterior surface of the maxilla. The displacement of the palato-maxillary arch that we observed during spitting resembles the unilateral motions of the palato-maxillary arch observed in most colubroids during prey transport (the 'pterygoid walk' of Boltt and Ewer, 1964). The early advance phase of medial jaw transport (to use the terminology for the pterygoid walk of Cundall and Greene, 2000) is characterized by protraction of the palato-maxillary arch coupled with a lateral rotation of the maxilla and palatine in the frontal plane. Furthermore, experimental evidence (e.g. Cundall, 1983; Kardong et al., 1986) has demonstrated that the M. protractor pterygoideus plays a key role in producing these palato-maxillary displacements during ingestion. Haas (1930) described how the palatine and maxilla rotate in the sagittal plane during medial jaw transport (the pterygoid walk) in *Naja*; his summary figure (fig. 21 in Haas, 1930) depicts displacements very similar to what we observed during spitting. The rotation of the palatine and maxilla is a common feature in one clade of elapids (the palatine erectors of McDowell, 1970), and was recently explored in some detail (Deufel and Cundall, 2004). In all their key features the displacements observed during spitting appear to be pronounced, bilateral, transport mechanics.

Observations of ingestion in our spitting cobras and analysis of video recordings of prey ingestion in *N. pallida* yield consistent evidence of medial jaw transport, but not displacements of the magnitude evident during spitting. It may be that concurrent bilateral activation of the M. protractor pterygoideus, rather than sequential unilateral activation as seen during ingestion, allows for greater displacement relative to the braincase. The present study examined only the M. protractor pterygoideus from among the palato-maxillary arch musculature. Previous studies of ingestion have suggested that the M. protractor pterygoideus, M. levator pterygoideus, M. retractor pterygoideus and the M. pterygoideus may all be active during the initial (protractive) displacements of the palato-maxillary arch (Cundall and Greene, 2000). Two of these muscles, the M. retractor pterygoideus and the M. pterygoideus, are antagonists of the M. protractor pterygoideus. The M. pterygoideus inserts on the distal ectopterygoid and the ectopterygoid/maxillary joint; activation of this muscle would limit rotation of the maxilla in the frontal plane. The more pronounced palato-maxillary displacements we observed during spitting may be produced by the M. protractor pterygoideus functioning independently of its normal (ingestive) antagonists.

With the exception of the exit orifice of the fang (Fig. 1), only subtle anatomical differences were found among the palato-maxillary arches of spitting and non-spitting cobras. No obvious morphological feature essential to the venom release during spitting was found in the palato-maxillary arch. It appears that rather than evolving a suite of morphological specializations for spitting, cobras have instead coopted and modified a motor action pattern employed for ingestion. The independent evolution of this behavior among multiple independent lineages, combined with reports of occasional specimens of non-spitting cobras that spit (e.g. Carpenter and Ferguson, 1977; Wüster and Thorpe, 1992) suggest that the palato-maxillary complex of the Najini is well suited to achieve the displacement of the fang sheath requisite for spitting.

We would like to thank A. Deufel who provided the video recordings of *Naja pallida* ingestion. We thank A. Resetar and H. Voris of the Field Museum of Natural History, J. Rosado and J. Hanken of the Museum of Comparative Zoology, and J. Wilson and G. Zug of the United States National Museum for the loan of the specimens examined in this study. E. Kochva kindly provided us with microscope slides of sections through the head of *Walterinnesia aegyptia*. L. Auerbach assisted in the construction of the spit detector used for this study. We thank C. Holliday for his comments on an earlier draft of this manuscript. This study was supported by N.S.F. grant (IBN-0129805) to B.A.Y.

References

Bogert, C. (1943). Dentitional phenomena in cobras and other elapids, with notes on the adaptive modification of their fangs. *Bull. Amer. Mus. Nat. Hist.* **81**, 285-360.

Boltt, R. and Ewer, R. (1964). The functional anatomy of the head of the puff adder, *Bitis arietans* (Merr.). *J. Morph.* **114**, 83-106.

Carpenter, C. C. and Ferguson, G. W. (1977). Variation and evolution of stereotyped behavior in reptiles. In *Biology of the Reptilia*, vol. 7 (ed. C. Gans and D. Tinkle), pp. 335-554. New York: Academic Press.

Cascardi, J., Young, B. A., Husic, H. D. and Sherma, J. (1999). Protein variation in the venom spat by the red spitting cobra, *Naja pallida* (Reptilia: Serpentes). *Toxicon* **37**, 1271-1279.

Cundall, D. (1983). Activity of head muscles during feeding by snakes: A comparative study. *Amer. Zool.* **23**, 383-396.

Cundall, D. and Greene, H. (2000). Feeding in snakes. In *Feeding: Form, Function, and Evolution in Tetrapod Vertebrates* (ed. K. Schwenk), pp. 293-333. New York: Academic Press.

Deufel, A. and Cundall, D. (2004). Prey transport in 'palatine-erecting' elapid snakes. *J. Morphol.* (in press).

Duvernoy, D. M. (1832). Mémoire sur les caractères tirés de l'anatomie pour distinguer les serpents venimeux des serpents non venimeux. *Ann. Sci. Nat.* **26**, 113-160.

Fairley, N. H. (1929). The dentition and biting mechanism of Australian snakes. *Med. J. Aust.* **1**, 313-327.

Freyvogel, T. and Honegger, C. (1965). Der 'Speiakt' von *Naja nigricollis*. *Acta Tropica* **22**, 289-302.

Gabe, M. and Saint-Girons, H. (1967). Données histologiques sur le téguement et les glandes épidermoïdes céphaliques des lépidosauriens. *Acta. Anat.* **67**, 571-594.

Greene, H. (1988). Antipredator mechanisms in reptiles. In *Biology of the Reptilia*, vol. 16 (ed. C. Gans and R. Huey), pp. 1-152. New York: Alan R. Liss, Inc.

Haas, G. (1930). Über die Schädelmechanik und die Kiefermuskulatur einiger Proteroglypha. *Zool. Jahrb.* **52**, 347-404.

Haas, G. (1973). Muscles of the jaws and associated structures in the Rhynchocephalia and Squamata. In *Biology of the Reptilia*, vol. 4 (ed. C. Gans and T. Parsons), pp. 285-490. New York: Academic Press.

Ismail, M., Al-Bekairi, A., El-Bedaiwy, A. and Abd-El Salam, M. (1993). The ocular effects of spitting cobras: I. The ringhals cobra (*Hemachatus haemachatus*) venom-induced corneal opacification syndrome. *Clin. Toxicol*. **31**, 31-41.

Jackson, K. (2003). The evolution of venom-delivery systems in snakes. *Zool. J. Linn. Soc*. **137**, 337-354.

Kardong, K. (1982). The evolution of the venom apparatus in snakes from colubrids to viperids and elapids. *Mem. Inst. Butantan.* **46**, 105-118.

Kardong, K., Dullemeijer, P. and Fransen, J. (1986). Feeding mechanism in the rattlesnake *Crotalus durissus*. *Amph. Rept.* **7**, 271-302.

Keogh, J. S. (1998). Molecular phylogeny of elapid snakes and a consideration of their biogeographic history. *Biol. J. Linn Soc.* **63**, 177-203.

Knight, A. and Mindell, D. P. (1994). On the phylogenetic relationship of the Colubrinae, Elapidae, and Viperidae and the evolution of front-fanged venom systems in snakes. *Copeia* **1994**, 1-9.

Kochva, E. (1978). Oral glands of the Reptilia. In *Biology of the Reptilia*, vol. 10 (ed. C. Gans and K. Gans), pp. 43-161. New York: Academic Press.

Kochva, E. (1987). The origin of snakes and evolution of the venom apparatus. *Toxicon* **25**, 65-106.

Luna, L. (ed.) (1968). *Manual of the Histological Staining Methods of the Armed Forces Institute For Pathology*. McGraw-Hill, New York. 258pp.

McDowell, S. B. (1970). On the status and relationships of the Solomon Island elapid snakes. *J. Zool. Lond.* **161**, 145-190.

Mitchell, S. (1861). Researches upon the venom of the rattlesnake: with an investigation of the anatomy and physiology of the organs concerned. *Smith. Cont. Know*. **12**, 1-145.

Pough, F., Andrews, R., Cadle, J., Crump, M., Savitzky, A. and Wells, K. (1998). *Herpetology.* Prentice Hall, New Jersey. 577pp.

Presnell, J. and Schreibman, M. (1997). *Humason's Animal Tissue Techniques.* Johns Hopkins University Press, Baltimore. 572pp.

Radovanovic, M. (1928). Der Giftapparat der Schlangen mit besonderer Berücksichtigung der *Naja tripudians*. *Jena. Z. Naturw*. **63**, 559-616.

Rasmussen, S., Young, B. A. and Krimm, H. (1995). On the 'spitting' behaviour in cobras (Serpentes: Elapidae). *J. Zool. Lond.* **237**, 27-35.

Rosenberg, H. I. (1967). Histology, histochemistry and emptying mechanism of the venom gland of some elapid snakes. *J. Morphol.* **122**, 133-156.

Savitzky, A. (1980). The role of venom delivery strategies in snake evolution. *Evolution* **34**, 1190-1204.

Slowinski, J., Knight, A. and Rooney, A. (1997). Inferring species trees from gene trees: a phylogenetic analysis of the Elapidae (serpentes) based on the amino acid sequences of venom protein. *Mol. Phyl. Evol.* **8**, 349-362.

Warrell, D. and Ormerod, L. (1976). Snake venom ophthalmia and blindness caused by the spitting cobra (*Naja nigricollis*) in Nigeria. *Am. J. Trop. Med. Hyg.* **25**, 525-529.

Wüster, W. (1996). Taxonomic changes and toxinology: systematic revisions of the Asiatic cobras (*Naja naja* species complex). *Toxicon* **34**, 399-406.

Wüster, W. and Thorpe, R. (1992). Dentitional phenomena in cobras revisited: spitting and fang structure in the Asiatic species of *Naja* (Serpentes: Elapidae). *Herpetol.* **48**, 424-434.

Young, B. A., Blair, M., Zahn, K. and Marvin, J. (2001a). Mechanics of venom expulsion in *Crotalus*, with special reference to the role of the fang sheath. *Anat. Rec.* **264**, 415-426.

Young, B. A., Daley, K. and Lee, C. (2001b). The comparative anatomy of the fang sheath in snakes. *Am. Zool.* **41**, 1633.

Young, B. A., Lee, C. E. and Daley, K. M. (2002). Do snakes meter venom? *BioScience* **52**, 1121-1126.

Young, B. A., Phelan, M., Morian, M., Ommundsen, M. and Kurt, R. (2003). Venom injection in rattlesnakes (*Crotalus*): Peripheral resistance and the pressure-balance hypothesis. *Can. J. Zool.* **81**, 313-320.

Young, B. A., Zahn, K., Blair, M. and Lalor, J. (2000). Functional subdivision of the venom gland musculature and the regulation of venom expulsion in rattlesnakes. *J. Morphol.* **246**, 249-259.

Zamudio K., Hardy, D., Martins, M. and Greene, H. (2000). Fang tip spread, puncture distance, and suction for snake bite. *Toxicon* **38**, 723-728.